Sādhanā (2023)48:184
https://doi.org/10.1007/s12046-023-02235-8

Investigation of combined natural convection and radiation in a square enclosure with a partition

MARIYAM ALI* and ANIL KUMAR SHARMA

Department of Mechanical Engineering, Faculty of Engineering and Technology, Jamia Millia Islamia (A Central University), New Delhi 110025, India
e-mail: alymariyam1318@gmail.com; asharma1@jmi.ac.in

MS received 31 January 2023; revised 25 May 2023; accepted 12 July 2023

Abstract. In this research paper, the results of the numerical investigations on combined surface radiation and natural convection heat transfer in a square enclosure with partition are presented. The vertical walls of the square enclosure are differentially heated, with the left wall at a higher temperature and the right wall at a lower temperature. The partition is placed parallel to these isothermal vertical walls while the horizontal walls are adiabatic. The simulation is done for a Rayleigh Number ranging between 10^3 and 10^6, Prandtl number of 0.7 (air). In this research work, the numerical simulation is carried out using the software ANSYS FLUENT 2022R1 in which the governing equations of fluid flow and heat transfer with surface radiation are solved using finite volume-based solver and coupled algorithm. Discrete Ordinate (DO) is used as the radiation model. The thickness of the partitioned is fixed and is equal to one twentieth of the length of the square enclosure. An analysis from the obtained streamlines, temperature contours and Nusselt number values shows the significant influence of surface radiation on natural convection heat transfer. It has been observed that increasing the length of partition reduces the Nusselt number, when the height of partition is varied from h = L to L/4, the value of Nusselt number increases to 7.2% for Ra 10^3 and 30.3% for Ra 10^6. It is also established that increasing the distance of partition from hot wall increases the Nusselt number. Likewise, an increase in emissivity leads to an increase in total Nusselt number which can be noted that when emissivity is changed from 0.25 to 1, the increase in total Nusselt number is found to be 24.9% and 97.1% respectively when compared with pure convection for Ra = 10^3. For Rayleigh number 10^6 the increase in Nusselt number is 32.6% and 170.9% sequentially when compared with pure convection.

Keywords. Surface radiation; natural convection; partitioned enclosure.

1. Introduction

The investigation of fluid flow and heat transfer has been a focal point of research for the past few decades. Mostly for the purpose of various engineering applications like the design of solar collectors, energy transfer in rooms and buildings, electronic cooling, heat exchangers, boilers, furnace and nuclear equipment due to which the study of combined natural convection and radiation is requisite. However, with improved designs and equipment, enclosures with partitions have become quite popular among researchers. Nagaraja *et al* [1] in their research work performed a numerical simulation of natural convection inside a square cavity with partitions. The partitions were placed vertically protruding from the horizontal end walls and the height of the partitions was also changed for the study. In their analysis they concluded that the overall heat transfer rate decreases with an increase in partition height and also due to decrease in length of location of partition. Almakhyoul *et al* [2] studied the effect of staggered non-conductive partitions on natural convection heat transfer in three different shaped cavities rectangular, trapezoidal, and triangular and they performed the numerical simulation using finite difference technique to solve continuity, momentum and energy equations. Similar to the observations of Nagaraja *et al* and Almakhyoul *et al* concluded that the increase in the length of the partition decreases the rate of heat transfer and Nusselt number. Another important observation made by them was that for the same length of partition the Nusselt number decreases in the order from rectangular to trapezoidal to triangular.

Parmananda *et al* [3] performed a numerical computation of combined natural convection and radiation in a cubical enclosure in order to study the effect of partition placed inside the enclosure. The study was carried out by placing the partition at four different positions. Natural convection in a square enclosure with partition having a fluid-saturated porous medium with internal heat generation was studied

*For correspondence
Published online: 23 August 2023

by Selamat and Ishak Hashim [4]. They considered two thin partitions for the analysis which were fully insulated. As such the effects of the position of the partitions on natural convection was studied. Sathiyamoorthy and Chamka [5] used the finite element method to study the effect of a very thin partition attached at the bottom wall of a square cavity having free convection within the cavity. The square cavity considered was heated from the bottom, had linearly heated side walls and the top wall been adiabatic and the analysis was done to study the effect of thin partition on Rayleigh–Benard instability. Two types of partitions were considered for the analysis, (i) highly conducting and (ii) insulating; with different lengths and positions. Suvash and Gu [6] carried out a numerical simulation for Natural Convection heat transfer in an isosceles triangular enclosure in which a partitioned vertical wall was placed at the centre of the enclosure and the thermal conductivity of the partition was considered to be infinite. In order to study the transient behaviour of the air flow and heat transfer, it was observed by the researchers that the coupled thermal boundary layer development around the partition undergoes several stages like an initial stage, a transition stage, and a steady stage. Yamaguchi *et al* [7] used a finite volume method to carry out a numerical simulation of natural convection heat transfer inside a three-dimensional enclosure and to study the effect of partition wall on natural convection in a vertical air layer. The partitions considered for the analysis in this research work were of finite thickness and of finite thermal conductivity. Various boundary conditions were considered for the analysis such as conduction, adiabatic and no thickness partitions and the results for all of the different boundary conditions were compared and were presented in the form of overall heat transfer and average Nusselt number.

Bilgen [8] carried out a numerical simulation to study the effect of partial partition in a two-dimensional enclosure. Various geometrical parameters like the aspect ratio, partition position and partition height were varied for the analysis. The researchers concluded that the rate of heat transfer decreases (i) when two partitions were used instead of one, (ii) when the aspect ratio was made smaller and (iii) when the position of partition wall was farther away from hot wall. Khalifa and Khudheyer [9] carried out an experimental investigation in a cavity having an aspect ratio of 0.5 to study natural convection and to study the effect of 14 different arrangements of partition inside the cavity. Air was considered as the working fluid to perform the experiment and the Rayleigh number ranged from 6×10^7 to 1.5×10^8. However, from the previous studies on natural convection inside a differentially heated partitioned enclosures, it can be seen that the radiation effect is often neglected. This could result in over simplification of the considered problem and can lead to a substantial inaccuracy in the results. Ramesh et al [10] used an optical device namely the differential interferometer (DI) to study the effect of partition thermal resistance and also the effect surface radiation and natural convection on total heat transfer between vertical walls of the partition enclosure in an experimental procedure. In this paper, the researchers evaluated the value of average Nusselt number for two different partition materials i.e., pure copper and Teflon for increasing values of Rayleigh number. Karki *et al* [11] numerically investigated the effect of partition placed parallel to the vertical isothermal walls in a cubic enclosure having free convection. The partitions along with the horizontal walls were assumed to be adiabatic. The width of the opening in the partition was kept constant while the height was varied from 0.25 to 0.75 of the enclosure heights. The results were obtained in the form of average Nusselt number and were also compared with the results obtained from cavities having similar arrangement in two-dimension. The observation made was that the average Nusselt numbers for three-dimensional enclosures are 15–66 percent smaller than those for two-dimensional enclosures with the same relative opening height.

Ciofalo and Karayiannis *et al* [12] did a numerical and experimental study of natural convection in a rectangular enclosure and presented in their research work, the effect of partitions projecting centrally from the end walls of vertical cavity on heat transfer rates. In their research work they analysed the effects of different thermal boundary conditions at the end walls and at the partition in a non-partitioned and partitioned enclosure. Khatamifar *et al* [13] studied the conjugate natural convection heat transfer in a square enclosure with a partition of finite thickness and conductivity in the transient state over a Rayleigh number range of 10^3 to 10^8. In this research work they observed that the effect of thermal conductivity ratio on heat transfer and fluid flow is insignificant when the thermal conductivity ratio is very large (100 or more) and is effective only when the ratio is between 0.1 and 10. They also concluded that the effect of partition thickness is only significant when the conductivity ratio is small. Nansteel and Grelf [14] studied the phenomenon of natural convection in a two-dimensional rectangular enclosure first without a partition and then with a partition. The partition was projecting vertically from the top adiabatic horizontal wall. The investigation was done experimentally with water being taken as the working fluid. Dye-injection flow visualization and thermocouple probes were used to observe the effect of the partial vertical divisions on the fluid flow and temperature fields respectively. The results in the form of Nusselt number for different Rayleigh number and partition length were presented for both conducting and non-conducting partition materials. Kahveci *et al* [15] used polynomial based differential quadrature (PDQ) method to study the effect of heat conducting vertical partition placed in an enclosure for natural convection. The results were presented in the form of streamlines, isotherm contours and Nusselt number.

Therefore, the present study deals with the combined effects of laminar natural convection and radiation in a

square cavity with partitions of different stature and positions.

1.1 *Governing equations*

The physics inside the enclosure is governed by the following set of equations (Bejan [16]):

Continuity Equation:

$$\frac{\partial u}{\partial x}+\frac{\partial v}{\partial y}=0 \tag{1}$$

x—Momentum Equation:

$$\rho\left(u\frac{\partial u}{\partial x}+v\frac{\partial u}{\partial y}\right)=-\frac{\partial p}{\partial x}+\mu\left[\frac{\partial^2 u}{\partial x^2}+\frac{\partial^2 u}{\partial y^2}\right] \tag{2}$$

y—Momentum Equation:

$$\rho\left(u\frac{\partial v}{\partial x}+v\frac{\partial v}{\partial y}\right)=-\frac{\partial p}{\partial y}+\mu\left[\frac{\partial^2 v}{\partial x^2}+\frac{\partial^2 v}{\partial y^2}\right]+\rho\beta g\Delta T \tag{3}$$

Energy Equation:

$$\rho C_p\left(u\frac{\partial T}{\partial x}+v\frac{\partial T}{\partial y}\right)=K\left[\frac{\partial^2 T}{\partial x^2}+\frac{\partial^2 T}{\partial y^2}\right] \tag{4}$$

1.2 *Coupling between Natural Convection and Surface Radiation*

The computation domain is enclosed by wall and inbuilt with partitions and therefore, multiple radiation reflections take place from all the surfaces. To evaluate the respective wall temperatures from the radiation model considered in analysis, the local values of respective heat transfer coefficients and fluid temperature are to be obtained from the flow calculations. The coefficient of heat transfer h is evaluated as $k_f/\Delta y$. The wall surfaces are considered as gray, opaque, and diffuse. Based on these assumptions, the generalized energy balance equation for all the walls is derived as follows (Siegel and Howell [17]):

$$h_1(T_1-T_w)+h_2(T_2-T_w)+\varepsilon_1 I_1+\varepsilon_2 I_2=(\varepsilon_1+\varepsilon_2)\sigma T_w^4 \tag{5}$$

where T_1 and T_2 are local values of fluid temperature, T_w is wall temperature, h is heat transfer coefficient, ε is emissivity of the wall surface, and I is the irradiation falling on the wall surface. The subscripts *2* and *1* refer to conditions on inner side and outer side of the enclosure. For the isothermal hot wall, h_1 is set to a large value with $T_1 = T_h$, and $\varepsilon_1 = 0$. Similarly, for the isothermal cold wall, h_1 is set to a large value with $T_1 = T_c$ and $\varepsilon_1 = 0$. For these walls the enclosure side heat transfer coefficient, $h_2 = k/\Delta x_w$. For the adiabatic walls, $h_1 = \varepsilon_1 = 0$ and $h_2 = k/\Delta y_w$. In these, Δx_w and Δy_w are the distances of the first fluid node from the wall. The irradiation is related to radiosity (B),

$$B_i=\varepsilon_i\sigma T_{wi}^4+(1-\varepsilon_i)I_i \tag{6}$$

where the subscript i is the index of the elemental segment forming the enclosure. There are N (equal to $N_x \times N_y$) elemental segments in the enclosure, where N_x and N_y are the number of elements in the x and y directions. Substituting for I in terms of B and using the inverse relationship,

$$I_i=\sum_{j=1}^{N}B_j F_{i-j} \tag{7}$$

and

$$\sum_{j=1}^{N}\left[\frac{\delta_{i,j}-(1-\varepsilon_i)F_{i-j}}{\varepsilon_i}\right]B_j=\sigma T_i^4 \tag{8}$$

where, $F_{i\text{-}j}$ is shape factor from segment i to segment j.

2. Physical model and problem description

Figure 1 shows the geometry of the physical model schematically. The length of the square cavity is taken as L with a vertical partition placed parallel to the hot and cold walls. The thickness of the partition is considered to be equal to one twentieth of the width of the square enclosure, t = L/20. The distance of the partition from the hot wall is varied as S_P L/4, L/2 and 3L/4 as designated by C(a), C(b) and C(c) respectively. Similarly, the height of the partition is changed as in h = L, 3L/4, L/2 and L/4 as shown in figure 1 by C(1), C(2), C(3) and C(4) respectively. The left vertical wall of the square cavity is considered at higher temperature T_h and right wall at lower temperature T_c and

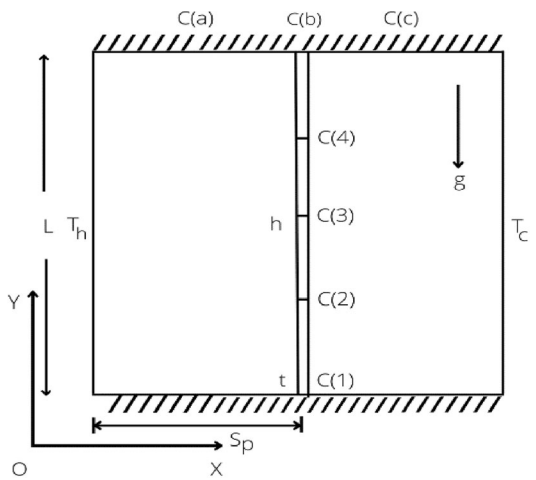

Figure 1. Computational domain.

the top and bottom horizontal walls are assumed to be adiabatic. The temperature difference between the hot and cold wall is taken as 20K. The fluid considered for the analysis is air having a Prandtl number of 0.7. Air is non-emitting and non-absorbing under normal temperature conditions which in turn make it a radiatively non-participating medium. The cavity walls and partitioned surfaces are assumed to be opaque, gray and diffuse emitters and reflectors of radiation with an emissivity ε. The gravity g acts downward normal to the x direction. Certain assumptions are made for the fluid flow for the numerical simulation such as the fluid flow is considered to be two-dimensional, incompressible, steady and laminar. The thermos-physical properties of the fluid in the flow model are assumed to be constant except for the density variation causing a body force term in the momentum equation. The Boussinesq approximation is assumed to be valid. Also, it is assumed that there is no slip wall surface.

2.1 *Solution methodology*

The numerical simulation for the present study is done using ANSYS FLUENT 2022R1. The continuity, momentum and energy equations are solved using finite volume method. The pressure velocity coupling is carried out by Coupled algorithm and Second order scheme is used for pressure interpolation. Second Order Upwind is adopted for momentum and energy equation, while First order Upwind is used for radiation equation. Surface radiation is invoked on the walls of the enclosure. The shape factor is evaluated using Hottel's cross-string method. The value of surface emissivity for all the considered cases is taken as one, i.e., ε = 1.

3. Grid independence test

The Grid Sensitivity Analysis has been carried out for the case 1b (h = L; S_P = L/2). Five grid sizes have been chosen for the analysis, namely 50 × 50, 100 × 100, 200 × 200, 400 × 400 and 800 × 800 for Rayleigh number 10^6. From Table 1 it can be observed that the changes between the results for the grid sizes is very nominal, as such 100 × 100 grid size mesh has been chosen for the analysis.

Table 1. Grid sensitivity study for different grid sizes for Rayleigh number 10^6.

Grid	Nu (numerical)	% Change with Numerical results
50 × 50	12.061	–
100 × 100	11.977	0
200 × 200	11.972	0.696
400 × 400	11.601	0.041
800 × 800	11.656	− 0.474

4. Results and discussion

In order to enumerate the combined effect of natural convection and radiation in a differentially heated partitioned square cavity, the results are demonstrated with the help of streamline, temperature contours and the total average Nusselt number for the considered range of Rayleigh number i.e., 10^3–10^6. The effect of emissivity, Rayleigh number, partition height and its distance from the hot wall are studied extensively. For the purpose of this investigation the partition thickness and thermal conductivity are kept constant. Four different cases 1, 2, 3 and 4 are considered in the present study with their subdivisions as a, b and c taken as shown in figure 1.

For all the cases the boundary conditions of the enclosure remain same i.e., left vertical wall is the hot wall, right wall is the cold wall and the top and bottom walls of the enclosure are adiabatic as described in previous section. In case 1 the height of the partition is taken as h = L. For case 2 the height of the partition is considered as h = 3L/4 maintaining a gap of L/4 between the bottom horizontal wall and the partition. For case 3 two partitions are considered, one protruding from the top horizontal wall and the other from the bottom horizontal wall. The height of the partition attached to the top wall is L/2 while the height of the partition attached to the bottom wall is L/4 keeping a gap between them as L/4. Case 4 corresponds to the inverse situation where the height of the partition attached to top wall as L/4 and height of partition attached to bottom wall as L/2 maintaining a gap of L/4 between the top and bottom partition. In all the cases the subdivisions a, b and c correspond to the situations where the partition distances from the hot wall are L/4, L/2 and 3L/4, respectively.

For the present study, the experimental results obtained by Bajorek [18] on natural convection in partitioned enclosures have been validated. From the graph as shown in figure 2 it can be seen that results of present study confirm with the experimental results of Bajorek.

Table 2 demonstrates the comprehensive validation results of average Nusselt number for natural convection for present study which are being compared by the results of Khatamifar *et al* [13] and Kahveci *et al* [15]. Foregoing validation results show that the Nusselt number obtained for Rayleigh number 10^3–10^6 agree.

4.1 *Pure natural convection*

To study the effect of pure natural convection in a partitioned cavity, a particular situation is selected where the Rayleigh number is considered as 10^4, with different cases 1, 2, 3 and 4 with their sub-categories as a, b and c. Figure 3 represents the streamlines and temperature contours for all the above-mentioned cases. In figure 3a, d, g and j for case 1a, 2a, 3a and 4a, respectively when the partition is near the hot vertical wall, it can be observed from the streamline

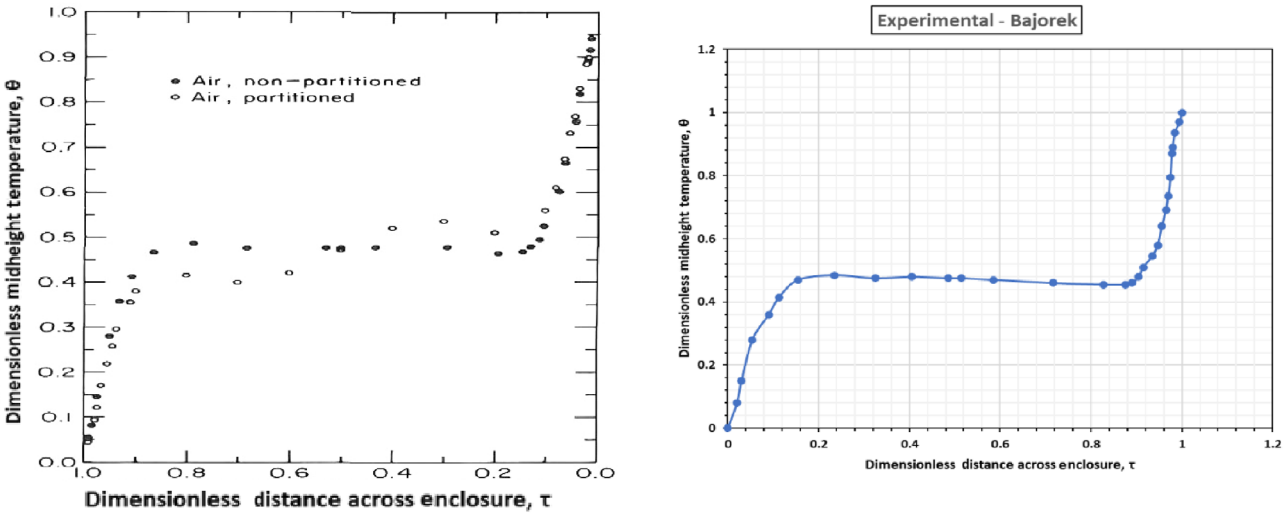

(**a**) Midheight temperature profile at Gr_w 10^5 for Bajorek exp. work (**b**) Present work for Ra = 10^5

Figure 2. Graph of comparison between experimental results of Bajorek [18] with the numerical simulation results for present study for validation.

Table 2. Comparison of hot wall average Nusselt number for different Rayleigh number range for partitioned square cavity.

Ra	Present study	M. Khatamifar et al	% Deviation	K. Kahveci et al	% Deviation
10^3	1.05	–	–	–	–
10^4	1.12	1.17	4.27	1.19	5.88
10^5	1.99	2.11	5.68	2.08	4.32
10^6	3.87	4.03	3.97	3.92	1.27

that the flow field is present at the right side of the partition. The fluid near the right bottom end of the partition rises to the top end then comes in contact with the top horizontal adiabatic wall which then flows in the downward direction along the cooled right vertical wall. Again, fluid moves upward as soon as it comes in contact with right side of the partition which results in the clockwise rotation of the fluid flow. It is also evident from the isotherm contours that are parallel to hot and cold walls and also near the partition however they form smooth curves at the right side of the partition as we move away from the partition and cold walls. Moreover, from the graph in figure 4 it is also clear that the value of average Nusselt number for case 1a, 2a, 3a and 4a for hot wall is close to 1.4.

For cases 1b, 2b, 3b and 4b in figure 3b, e, h and k respectively when the partition is present at the centre it is seen from the streamline contours that the fluid in contact with the hot wall rises up from the bottom end then comes in contact with the partition wall which deflects it in the downward direction forming clockwise rotation of fluid. Similar situation occurs on the right side of the partition, which results in flow field on both the sides of the partition wall and only a small interaction occurs between these two fluid flow parts. The temperature contours also clearly depict that the contours are nearly parallel to the hot, cold and partition walls. Similarly, from the graph in figure 4 it is also clear that the value of average Nusselt number for case 1b, 2b, 3b and 4b for hot wall is close to 1.1. The streamline contours for cases 1c, 2c, 3c and 4c in figure 3c, f, i and l when the partition is close to the cold wall shows that the flow field is present on the left side of the partition wall. The fluid present near the bottom end of hot wall rises up along the hot wall to the top end and then moves downward as soon as it comes in contact with the left side of the partition wall. Again, moves upward as it comes in contact to the bottom end of hot wall forming clockwise fluid flow rotation. Also, the temperature contours are parallel to the vertical walls while forming smooth curves at the left side of the partition wall. Likewise, from figure 4 the graph clearly shows that the value of average Nusselt number for cases 1c, 2c, 3c and 4c is nearly equal to 1.4.

Figure 4 shows that the value of Nusselt number for natural convection lies between 1.1 to 1.4, least at the centre when the partition of height h = L is placed at the centre and most when the partitioned is positioned farthest from the hot wall i.e., S_P = 3L/4 and the height of upper partition is L/4.

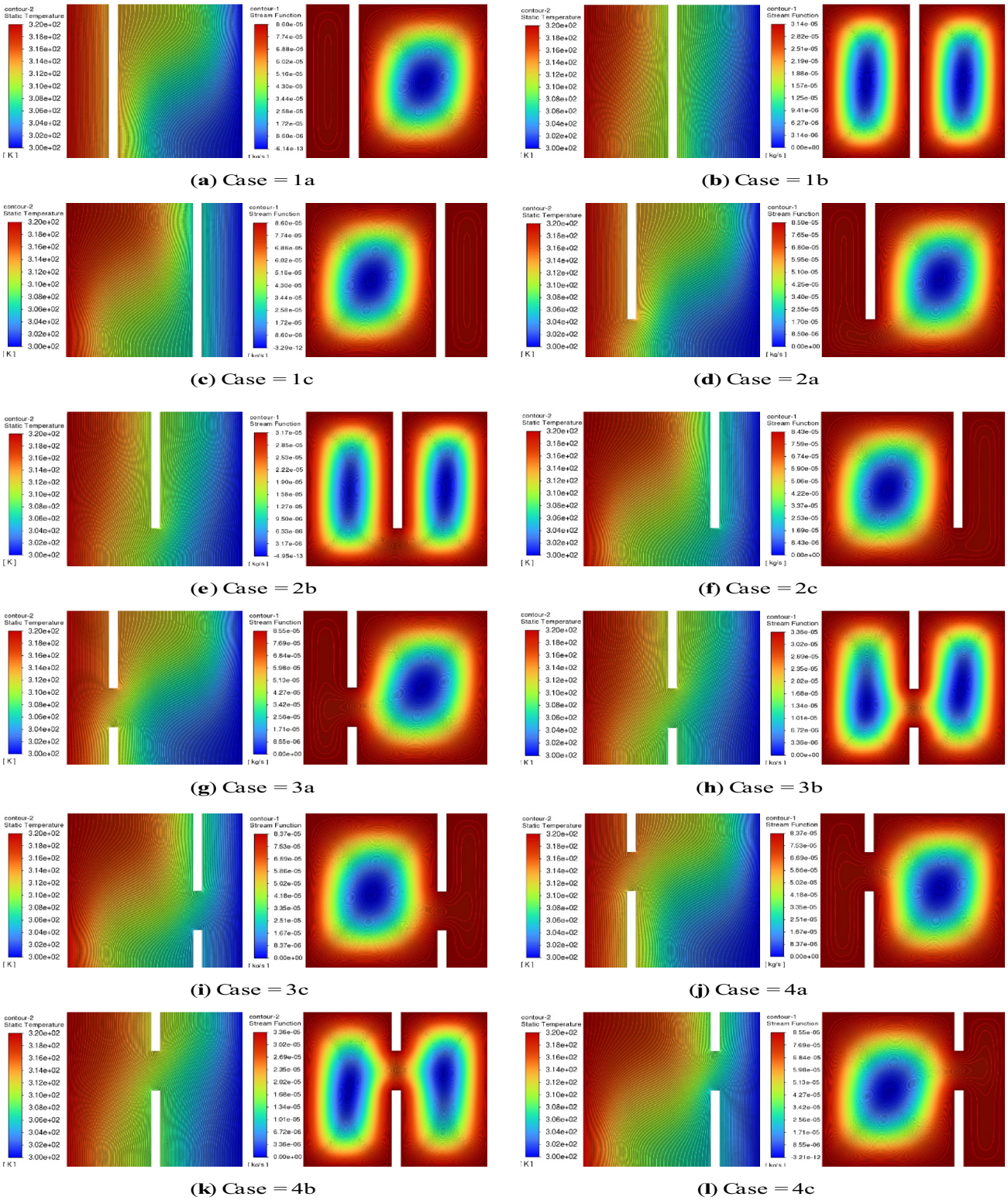

(a) Case = 1a **(b)** Case = 1b

(c) Case = 1c **(d)** Case = 2a

(e) Case = 2b **(f)** Case = 2c

(g) Case = 3a **(h)** Case = 3b

(i) Case = 3c **(j)** Case = 4a

(k) Case = 4b **(l)** Case = 4c

Figure 3. Temperature and Streamline Contours for natural convection for Rayleigh number 10^4 for all cases of partition height and distance from hot wall.

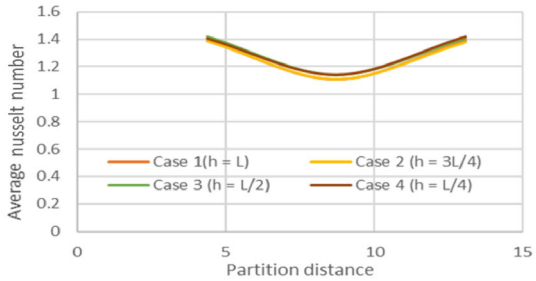

Figure 4. Variation of Average Nusselt number for natural convection with partition distance from hot wall for all cases of partition height for hot wall for Rayleigh number 10^4.

4.2 *Combined radiation and natural convection*

The combined natural convection and radiation phenomenon within a differentially heated square cavity with partition is presented for Rayleigh number ranging from 10^3 to 10^6, Pr = 0.7 and emissivity ε = 1 with help of temperature, streamlines contours and Nusselt number. With the inclusion of surface radiation, the nature of the flow and temperature distribution gets distorted leading to a change in heat transfer phenomenon which can also be observed from figures 9, 10, 11 and 12 where the graph shows that the value of total Nusselt number is more than double that in pure convection.

The temperature and streamline contours for all the considered cases of partition height and distance from hot wall for Rayleigh number 10^3 is shown in figure 5. From the streamline contours for all the Rayleigh number, it is observed that the flow field is present on the right side of the partition having clockwise rotation of fluid flow for case 1a as can be observed from figures 5, 6, 7 and 8. For Ra = 10^3 in figure 5a the fluid near the right bottom end of the partition rises up to the top end then comes in contact with the top horizontal adiabatic wall which then flows in the downward direction along the cooled right vertical wall. Again, fluid moves upward as soon as it comes in contact with right side of the partition which results in the clockwise rotation of the fluid flow. It is also evident from the isotherm contours that are nearly parallel to the vertical walls in figure 5a. Even for Ra = 10^4 in figure 6a the flow field is present on the right side of the partition having a clockwise rotation. Also, the temperature contours are parallel very close to the hot, cold and partition walls and starts forming smooth curve at the centre of the cavity. The flow fields for Ra = 10^5 as shown in figure 7a shows similar behaviour as for Ra = 10^3 and 10^4 as shown in the streamline contours. However, for Ra 10^6 weak flow field is also present on the left side of the partition along with the flow field on the right side of the partition. The isotherm contours start deforming for Ra = 10^5 in figure 7a and nearly becomes parallel to the horizontal walls for Ra 10^6 in figure 8a of the enclosure at the right side of the partition.

The temperature and Streamline contours for Case 1b (h = L and S_P = L/2) for considered range of Rayleigh number i.e., 10^3–10^6 is presented in figures 5–8b respectively. From the streamline contours for Rayleigh number 10^3 to 10^6 it is observed that there are two flow fields formed separately on both the sides of the partition. On the left side of the partition the fluid rises from the bottom end of the hot wall, then comes in contact with the top horizontal adiabatic wall and then flows downward along the left side of the partition. Likewise, on the right side of the partition the fluid moves downward along the cold wall from the top end to the bottom end, then comes in contact with the bottom horizontal wall and further moves upward along the right side of the partition. This results in the clockwise rotation of fluid flow on both the sides of the partition. The isotherm contours for Rayleigh number 10^3 and 10^4 are parallel to the vertical sides of the cavity as displayed in figures 5–6b respectively. For Ra 10^5 in figure 7b the contours get distorted near the bottom end and top end of the hot and cold wall and also near the partition wall. As the circulation becomes stronger at the extreme ends when Ra = 10^6 in figure 8b it is observed that the isotherm contours get distorted which results in the central portion of contours becoming horizontal on both the sides of the partition. Figures 5–8c show the temperature and streamline contours for h = L, S_P = 3L/4 for the considered range of Rayleigh number i.e., 10^3–10^6 which is exactly similar to that of case 1a as can be referred from figures 5–8a. The only difference being the flow field present on the left side of the partition. Also, the isotherm contours show impeccable similarity with the temperature contours for case 1a.

The streamline and temperature contours for case 2a when the height of the partition is 3L/4 and the distance of partition is L/4 for Rayleigh number 10^3, 10^4, 10^5 and 10^6 are shown in figures 5–8d. For Ra = 10^3 and 10^4 as shown in figures 5–6d the flow fields are present only on the right side of the partition. The fluid rises near the bottom end of the partition, moves along the top horizontal adiabatic wall, gets deflected towards the right vertical cold wall and then again moves along the right side of the partition thus causing clockwise fluid rotation. It is also evident from the isotherm contours for Rayleigh number 10^3 that are parallel to the vertical sides of the cavity. From figure 6d even for Ra = 10^4 the contours are parallel very close to the hot, cold and partition walls and starts forming smooth curve at the centre of the cavity. However, for Ra 10^5 from the streamline contours in figure 7d it is seen that weak currents are also present on the left side of the partition. As the Ra number reaches 10^6 the circulation currents become stronger resulting in flow fields on both the sides of the partition as shown in figure 8d. For Ra 10^5 the temperature contours get distorted near the bottom end of the partition. As the circulation becomes stronger at the extreme ends when Ra = 10^6 it is observed that the isotherm contours get completely distorted which results in the central portion of contours becoming horizontal.

In case 2b when the partition is present at the centre with height being 3L/4, various observations are made from the

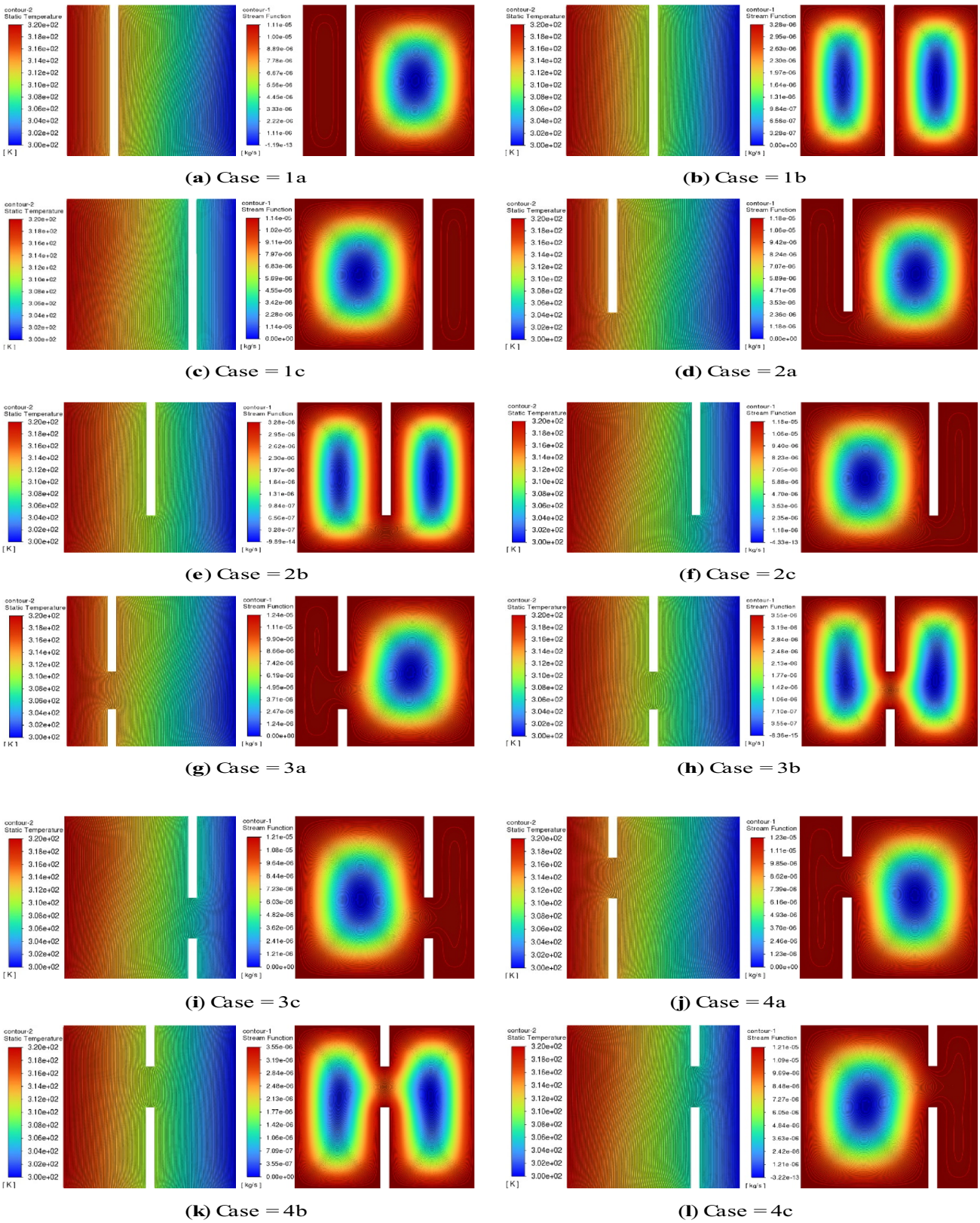

(a) Case = 1a **(b)** Case = 1b

(c) Case = 1c **(d)** Case = 2a

(e) Case = 2b **(f)** Case = 2c

(g) Case = 3a **(h)** Case = 3b

(i) Case = 3c **(j)** Case = 4a

(k) Case = 4b **(l)** Case = 4c

Figure 5. Streamlines and Temperature Contours for Rayleigh Number 10^3.

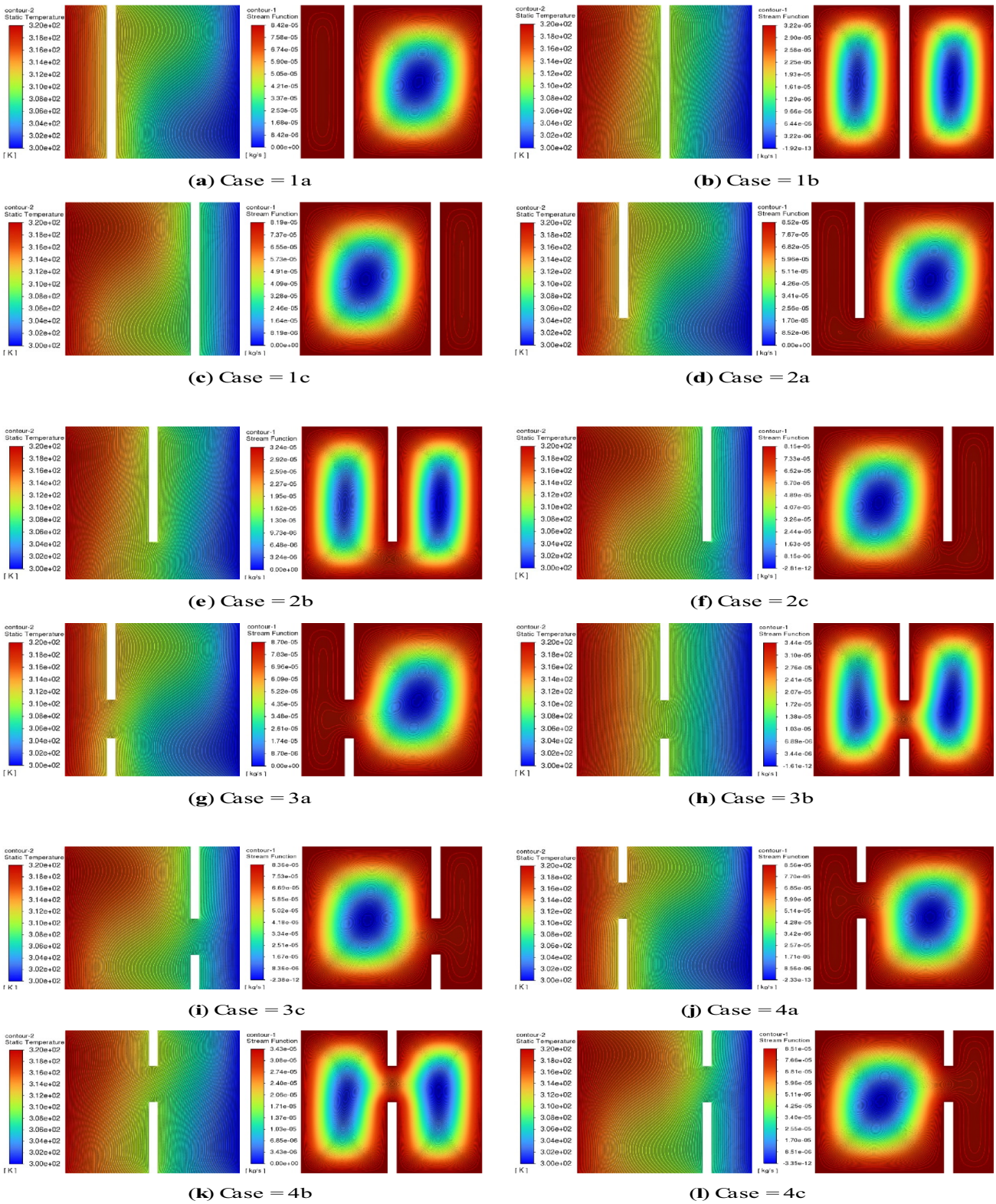

Figure 6. Streamlines and Temperature Contours for Rayleigh Number 10^4.

streamline and isotherm contours as shown in figures 5–8e. For Ra 10^3 and 10^4 the fluid rises from the bottom end of the hot wall and moves over it reaching to the top end as shown in figure 5e and figure 6e, respectively. As the

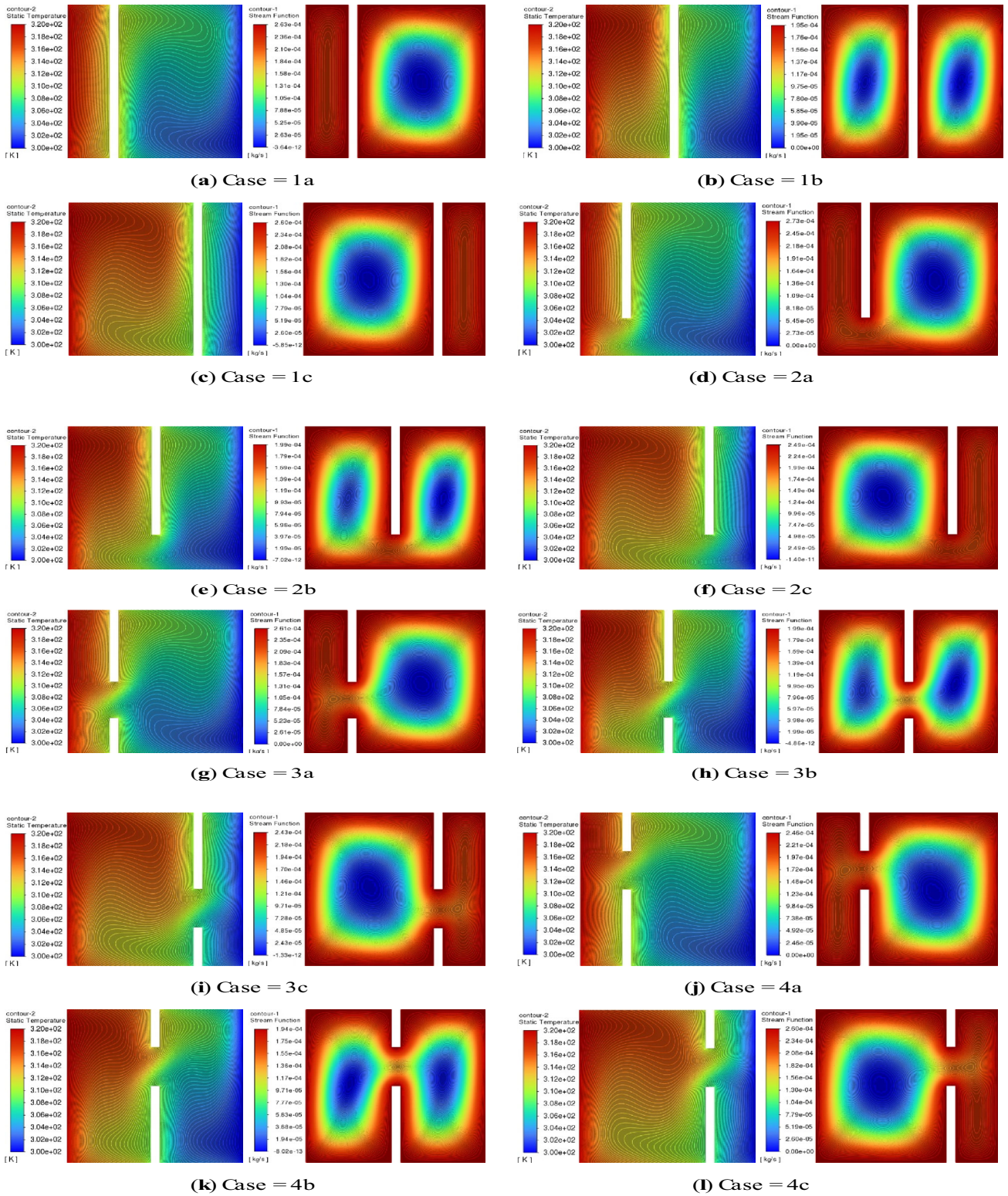

Figure 7. Streamlines and Temperature Contours for Rayleigh Number 10^5.

partition is projected from the top wall of the enclosure it deflects the fluid motion in the downward direction and again the fluid moves up as soon as it meets the bottom end of the hot wall. Similarly, on the right side of the partition the cold fluid moving along the cold wall in the downward direction, comes in contact with the bottom horizontal

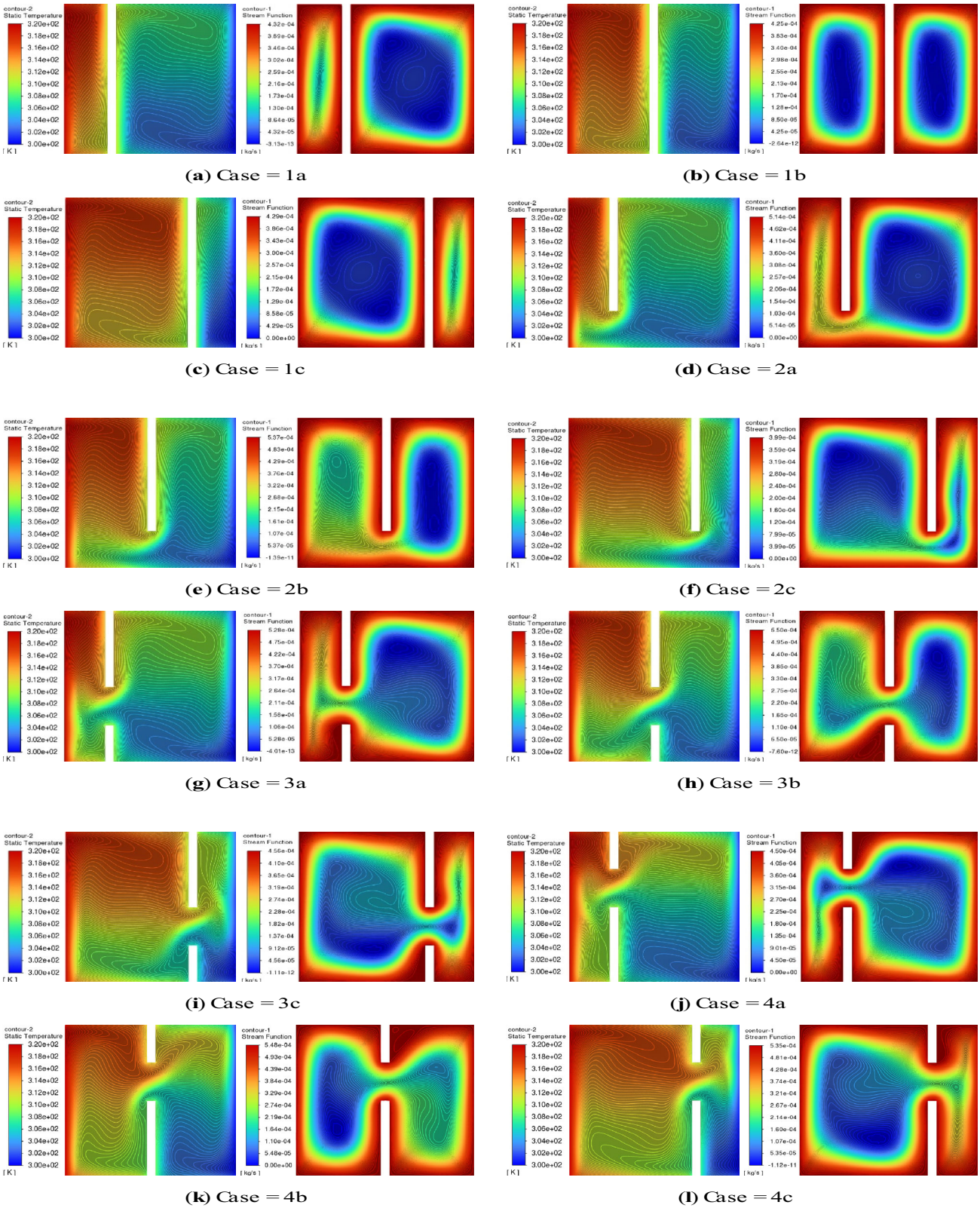

(a) Case = 1a **(b)** Case = 1b

(c) Case = 1c **(d)** Case = 2a

(e) Case = 2b **(f)** Case = 2c

(g) Case = 3a **(h)** Case = 3b

(i) Case = 3c **(j)** Case = 4a

(k) Case = 4b **(l)** Case = 4c

Figure 8. Streamlines and Temperature Contours for Rayleigh Number 10^6.

adiabatic wall and then moves up along the right side of the partition forming rolls with clockwise rotation on both the sides. Thus, two separate flow fields are formed on both the sides of the partition. It is also clear from the isotherm contours which are nearly parallel to the hot and cold wall for Ra = 10^3 and 10^4. Also, the total Nusselt number is greater than when radiation is neglected. For Ra 10^5 as shown in figure 7e the fluid moves along the hot surface in the upward direction, after coming in contact with the partition moves in the downward direction, then through the gap provided moves in the upward direction along the right side of the partition then flows over the top horizontal adiabatic wall and again after coming in contact with the cold wall moves in the downward direction hence causing a clockwise fluid flow motion inside the cavity. Similar flow fields form for Ra 10^6 but in this case the flow fields are much stronger as shown in figure 8e. For Ra 10^5 the temperature contours get distorted near the bottom end of the partition. As the circulations becomes stronger at the extreme ends when Ra = 10^6 it is observed that the isotherm contours get completely distorted which results in the central portion of contours becoming horizontal on right and left side of the partition respectively as shown in figure 8e.

Figures 5–8f show the streamline and temperature contours for case 2c when the height and distance of partition from hot wall is same i.e., 3 L/4 for Rayleigh number 10^3, 10^4, 10^5 and 10^6. From the contours a close resemblance is observed for case 2a and 2c, the only difference is the flow field is present at the left side of the partition for Ra 10^3 and 10^4 as shown in figure 5 and figure 6f respectively. It is also evident from the isotherm contours for Rayleigh number 10^3 that are parallel to the vertical sides of the cavity. Even for Ra = 10^4 the contours are parallel very close to the hot, cold and partition walls and starts forming smooth curve at the centre of the cavity. However, for Ra 10^5 from the streamline contours in figure 7f it is seen that weak currents are also present on the right side of the partition. As the Ra number reaches 10^6 the circulation currents become stronger resulting in flow fields on both the sides of the partition as shown in figure 8f. For Ra 10^5 the temperature contours get distorted near the bottom end of the partition. As the circulation becomes stronger at the extreme ends when Ra = 10^6 it is observed that the isotherm contours get completely distorted which results in the central portion of contours becoming horizontal on right and left side of the partition respectively.

The streamline and temperature contours for case 3a is shown in figures 5–8g where 2 partitions are considered, one attached to the top horizontal wall and the other to the bottom horizontal wall maintaining a gap of L/4 between them. The height of partition attached to top wall is L/2 while that attached to bottom wall is L/4. The distance between the hot wall and partition is taken as L/4. For Ra 10^3 as in figure 5g it is observed from the streamline contours that the fluid rises near the corner of the right side of the partition attached to the bottom horizontal wall then flows over the partition attached to the top horizontal wall, then after flowing over the top horizontal wall moves along the cold wall in the downward direction resulting in the clockwise rotation of fluid flow. Similar flow fields are observed in figure 6g for Ra 10^4. It is also clear from the isotherm contours for Ra 10^3 which are exactly parallel to the vertical wall. Though, for Ra 10^4 the isotherms are parallel only near the vertical walls and form smooth curves at the centre of the cavity. In case of Ra 10^5 in figure 7g it is seen from the streamline contours that the fluid moves along the hot surface in the upward direction, after coming in contact with the left side of the partition attached to top horizontal wall moves in the downward direction, then through the gap provided moves in the upward direction along the right side of the partition, then flows over the top adiabatic horizontal wall and again after coming in contact with the cold wall moves in the downward direction. Hence, after which the fluid flows over the bottom horizontal wall then flows over the partition attached to bottom wall after which moving over the partition flow over the hot wall in the upward direction resulting in the clockwise rotation of fluid flow. However, the flow field on the left side of the partition are very weak for Ra 10^5 when compared to the flow field for Ra 10^6. It is also clear from the isotherm contours for Ra 10^5 the contour gets distorted on the right side of the partition and for 10^6 the contour gets distorted and becomes parallel to the horizontal walls thus causing thermal stratification on the right side of the partition.

The streamlines and temperature contours for case 3b for the considered range of Rayleigh number i.e., 10^3–10^6 respectively is shown in figures 5–8h. The setup is like case 3a except for the partition distance from hot wall which in this case is taken as L/2. For Ra 10^3 and 10^4 two flow fields are present on both the side of partitions having a clockwise rotation of fluid flow as referred from figures 5 and 6h respectively. It is also clear from the isotherm contours for Ra 10^3 which are exactly parallel to the vertical wall. However, for Ra 10^4 the isotherms are parallel only near the vertical walls and form smooth curves at the centre of the cavity. Unlike for Ra 10^3 and 10^4 the flow fields on the right and left side of the partition for Ra 10^5 and 10^6 as demonstrated in figure 7h and figure 8h communicates through the gap between the top and bottom partitions. It is also clear from the isotherm for Ra 10^5 the temperature contours get distorted near the bottom end of the partition. As the circulations becomes stronger at the extreme ends when Ra = 10^6 it is observed that the isotherm contours get completely distorted which results in the central portion of contours becoming horizontal on right and left side of the partition respectively as shown in figure 8h. For Rayleigh number 10^3, 10^4, 10^5 and 10^6, figures 5–8i show the streamlines and temperatures contours for case 3c where the arrangement of partitions is similar to that in case 3a, the only difference being the distance of partition from hot

wall which in this case is 3 L/4. For Ra 10^3 from the figure 5i it is observed from the streamline contours that the fluid rises from the bottom end of hot wall to the top end, then flows over the top adiabatic horizontal wall then after flows along both the partitions in the downward direction resulting in the clockwise rotation of fluid flow. Similar flow fields are observed for Ra 10^4. It is also evident from the isotherm contours for Ra 10^3 which are exactly parallel to the vertical wall. However, for Ra 10^4 the isotherms are parallel only near the vertical walls and form smooth curves at the centre of the cavity as shown in figure 6i. In case of Ra 10^5, it is seen from the streamline contours that the fluid moves along the hot surface in the upward direction, after coming in contact with the left side of the partition attached to top horizontal wall moves in the downward direction, then through the gap provided moves in the upward direction along the right side of the partition, then flows over the top adiabatic horizontal wall and again after coming in contact with the cold wall moves in the downward direction. Hence, after which the fluid flows over the bottom horizontal wall then flows over the partition attached to bottom wall after which moving over the partition flow over the hot wall in the upward direction resulting in the clockwise rotation of fluid flow. However, the flow field on the right side of the partition are very weak for Ra 10^5 when compared to the flow field for Ra 10^6 as shown in figure 8i. It is also clear from the isotherm contours for Ra 10^5 the contour gets distorted on the left side of the partition and for 10^6 the contour gets distorted and becomes parallel to the horizontal wall.

For case 4a two partitions are considered the height of upper partition being L/4 and that of partition attached to bottom wall is L/2 maintaining a gap of L/4 between them and the distance of the partition from hot wall is L/4, the streamlines and temperature contours are shown in figures 5–8j. The streamline and temperature contours in this case are similar to that of case 3a which can be referred from figures 5–8i. For Ra = 10^3 and 10^4 the flow fields are present only on the right side of the partition. It is also clear from the isotherm contours for Ra 10^3 which are exactly parallel to the vertical wall. However, for Ra 10^4 the isotherms are parallel only near the vertical walls and form smooth curves at the centre of the cavity. For Ra = 10^5 and 10^6 weak flow fields are also present on the left side of the partition. It is also clear from the isotherm contours for Ra 10^5 the contour gets distorted on the right side of the partition and for 10^6 the contour gets distorted and becomes parallel to the horizontal walls thus causing thermal stratification on the right side of the partition. Figures 5–8k show the streamline and temperature contours for case 4b which are exactly similar to that of case 3b. Also, after comparing from the graphs in figures 11 and 12 for case 3b and 4b respectively for the values of Nusselt number, it is observed that the values are almost equal.

The streamline and temperature contours for case 4c are presented in figures 5–8 (l). The contours show immense similarity between case 3c and 4c. For Ra = 10^3 and 10^4 the flow fields are present only on the left side of the partition. It is also clear from the isotherm contours for Ra 10^3 which are exactly parallel to the vertical wall. However, for Ra 10^4 the isotherms are parallel only near the vertical walls and form smooth curves at the centre of the cavity as shown in figure 6(l). For Ra = 10^5 and 10^6 weak flow fields are also present on the right side of the partition. It is also clear from the isotherm contours for Ra 10^5 the contour gets distorted near the hot wall and the left side of the partition and for 10^6 the contour gets distorted and becomes parallel to the horizontal walls thus causing thermal stratification on the left side of the partition.

The graphs in figure 9 demonstrates the values of convective, radiative, and total Nusselt number for cases 1a, 1b and 1c. For Ra = 10^3 it is observed that the Nu_{cv} is more than the Nu_{rd} but from Ra = 10^4 onwards it is observed that the radiative Nusselt number is higher than the convective Nusselt number. The least value of total Nusselt number is noted for case 1b for all Rayleigh number range when the partition is present at the centre.

The values of radiative, convective and total Nusselt number for Rayleigh number 10^3, 10^4, 10^5 and 10^6 for cases 2a, 2b and 2c are presented in figure 10. It can be observed that the values of both convective and radiative Nusselt number is increasing as the Rayleigh number increases, Nu_{rd} increasing in higher proportion. This results in an increase of overall Nusselt number. For Ra 10^3 the value of Nu_{cv} is greater than Nu_{rd} while for rest of the Ra values Nu_{rd} is higher. Also, the least value of Nu_T is achieved when the partition is at the centre.

Figure 11 shows the values of convective, radiative and total Nusselt number for case 3. Similar to above cases, for Ra 10^3 Nu_{cv} is higher than Nu_{rd}. For Ra 10^3 and 10^4 least values of Nusselt number is observed when the partition is at centre while for 10^5 and 10^6 highest values of Nusselt number is observed at this location.

Figure 12 shows the values of convective, radiative and total Nusselt number for case 4. For Ra 10^3 Nu_{cv} is higher than Nu_{rd}. For Ra 10^3, 10^4 and 10^5 least values of Nusselt number are observed when the partition is at centre while for 10^6 highest values of Nusselt number is observed at this location.

4.3 *Effect of Rayleigh number*

The effect of Rayleigh number on combined natural convection and radiation inside a differentially heated partitioned square cavity is shown in figure 13. The graph shows the variation of Nusselt number with increasing Rayleigh numbers. The range of Rayleigh number considered is between 10^3 and 10^6. To study the effect of Rayleigh number the partition is considered at the centre i.e., S_P L/2. Also, the height of the partition is taken as h = L, 3 L/4, L/2 and L/4 respectively. It is clear from the graph that

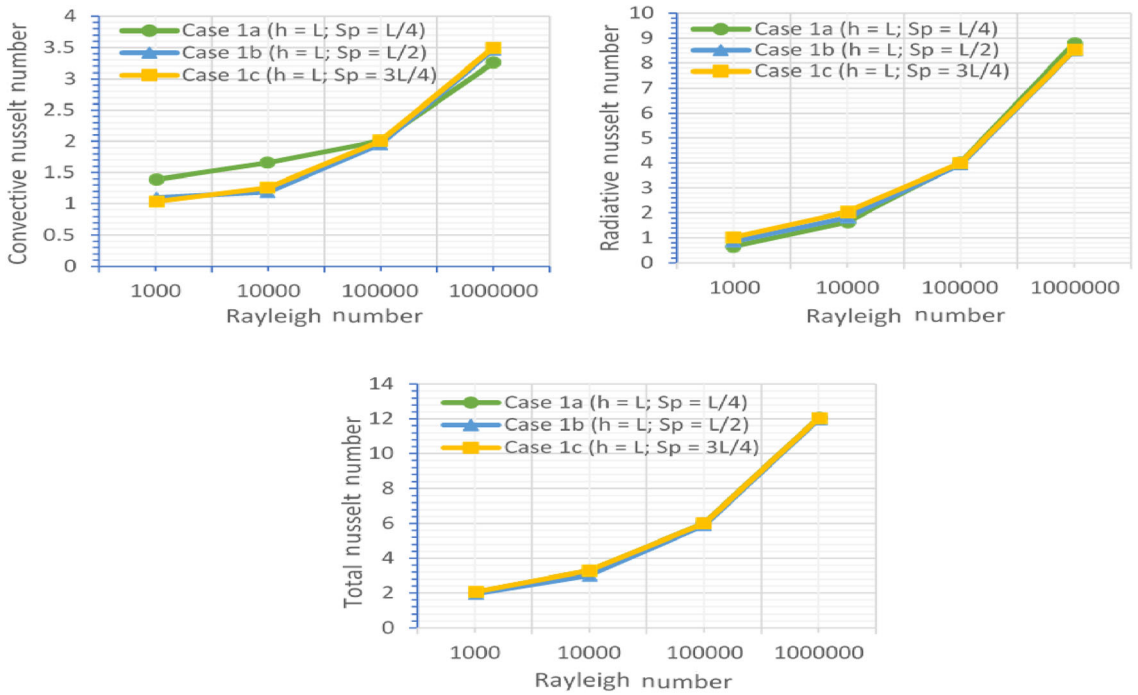

Figure 9. Variation of convective, radiative and total Nusselt Number for Combined natural convection and radiation for hot wall for ε = 1 in r case 1 for Rayleigh number ranging from 10^3 to 10^6.

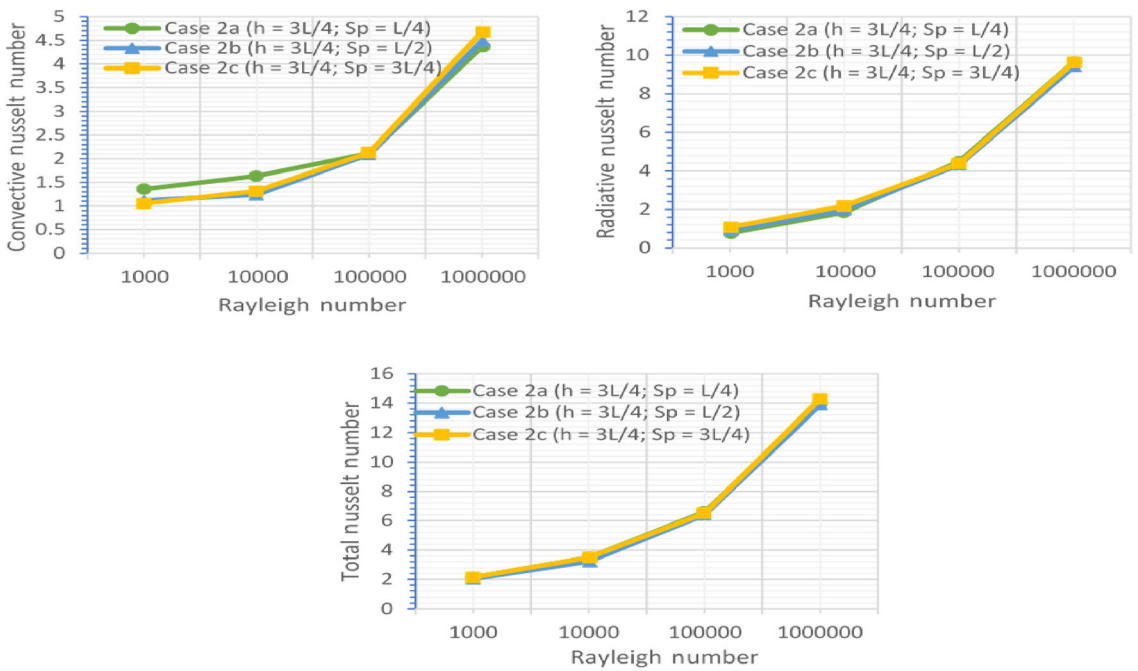

Figure 10. Variation of Total Average Nusselt Number for combined natural convection and radiation for hot wall for ε = 1 in case 2 for Rayleigh number ranging from 10^3 to 10^6.

increasing the Rayleigh number increases the overall heat transfer rate which further leads to an increase in Nusselt number. The maximum value of Nusselt number is observed when Ra is 10^6 while the least being at Ra = 10^3.

It is also evident from the streamline contours that when Ra = 10^3, the values of the flow field is very small and the transfer of heat occurs essentially by conduction. As the Rayleigh number increases to 10^5 the convection currents

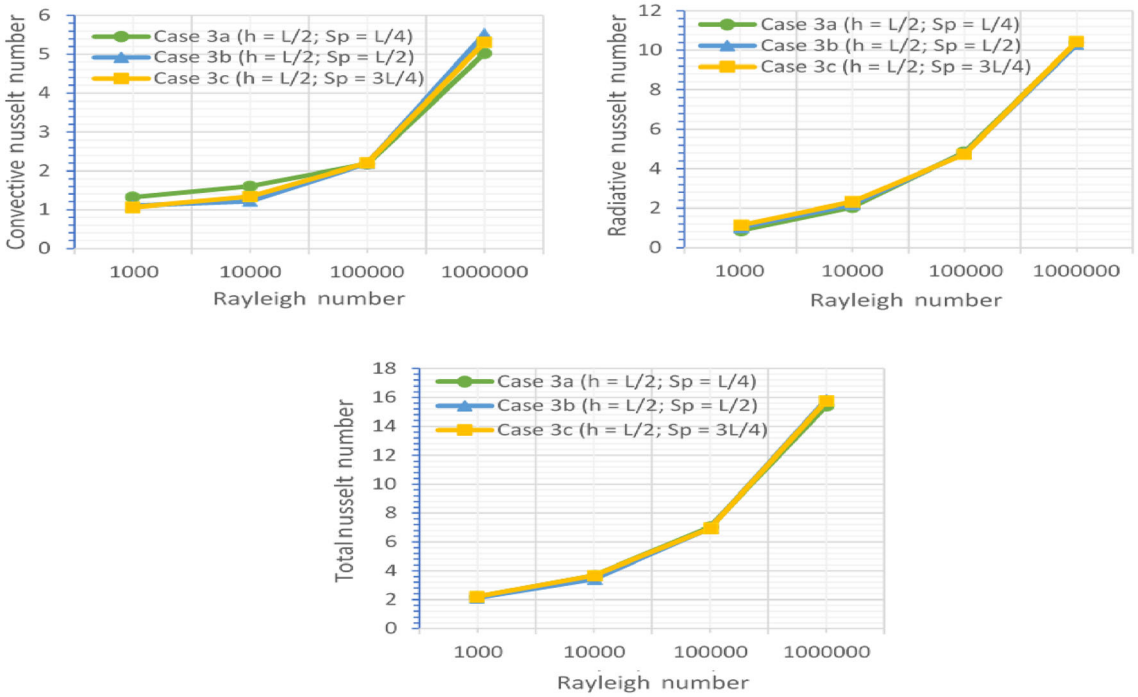

Figure 11. Variation of convective, radiative and total Nusselt Number for combined natural convection and radiation for hot wall for ε =1 in a differentially heated partitioned square cavity for case 3 for Rayleigh number ranging from 10^3 to 10^6.

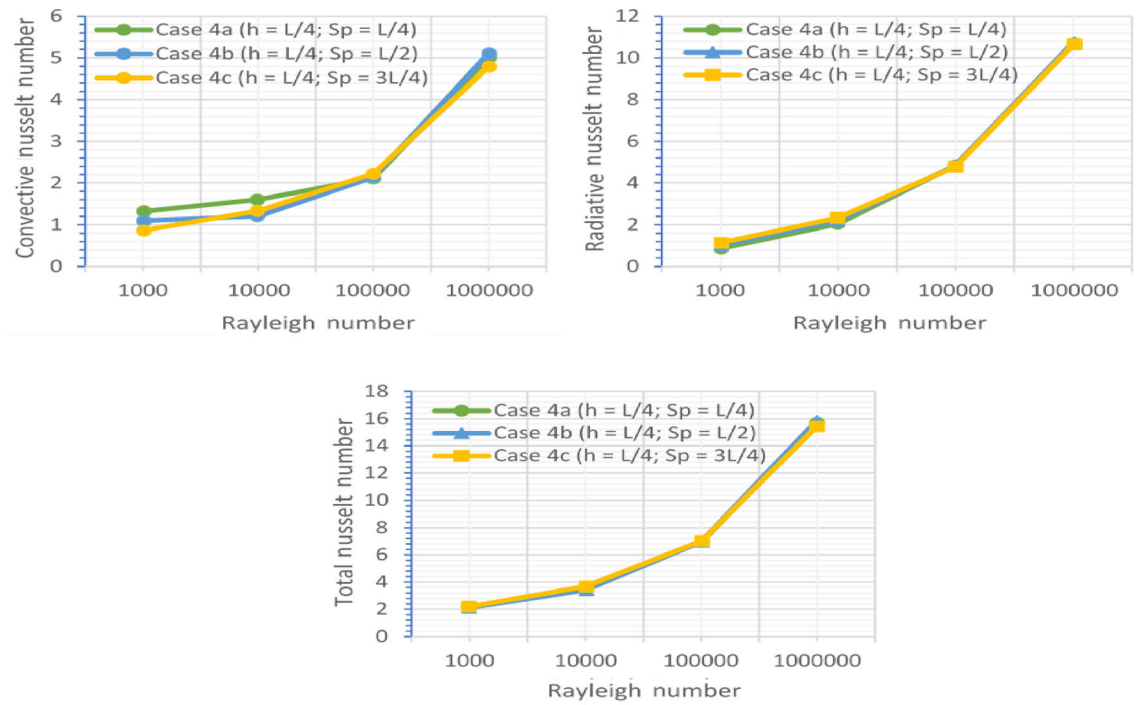

Figure 12. Variation of radiative, convective and total Nusselt Number for combined natural convection and radiation for hot wall for ε = 1 in case 4 for Rayleigh number ranging from 10^3 to 10^6.

and radiation currents become stronger leading to high rate of heat transfer and fluid flow. Further, increasing the Rayleigh number to 10^6 the effect of radiation dominates the transfer phenomenon which results in an increase in fluid flow. Also, the temperature contours are nearly parallel for Ra = 10^3 which happens due to weaker fluid flow

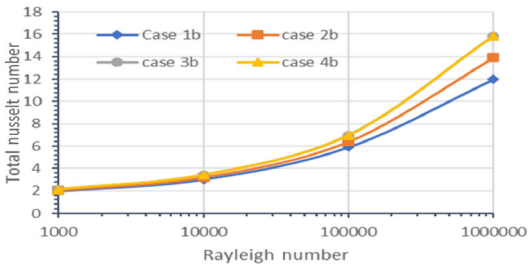

Figure 13. Variation of total Nusselt number with Rayleigh Numbers along the hot wall for central position of partition wall and different partition height.

and only starts forming smooth curve for Ra = 10^4. However, it is observed from the temperature contours that the fluid gets horizontally stratified when the Rayleigh number increases to 10^5. When the Rayleigh number reaches to a higher value of 10^6 it can be observed from the isotherm contours that the central portion of the contour is nearly horizontal except for the case when the partition is placed at the centre resulting in distorted contours near the bottom and top side of the hot and cold surfaces, respectively.

It is also clear from the graphs in figures 9, 10, 11 and 12 that the values of convective, radiative and total Nusselt number are presented for the Rayleigh number ranging from 10^3 to 10^6 for Prandtl number 0.7. It can be seen that as the Rayleigh number increases the value of convective, radiative and total Nusselt number increases. This happens because as the Rayleigh number is increased the effect of convection and radiation currents became stronger leading to higher values of Nusselt number.

4.4 *Effect of Emissivity*

In order to determine the effect of surface emissivity on heat transfer, the value of emissivity is changed as 0.25, 0.5, 0.75 and 1 for Rayleigh number 10^3 and 10^6 and the graphs are plotted between Radiative Nusselt number, Total Nusselt number and Emissivity below in figure 14 for cases 2a, 2b and 2c. It can be noticed from the graphs that as the value of emissivity is increased the value of Nu_{rd} and Nu_T increases linearly. This occurs due to higher thermal radiation emitted by surface having higher emissivity.

It is also observed that the inclusion of surface radiation decreases the convective Nusselt number. And this decrease in convective Nusselt number is compensated by the increase of radiative Nusselt number. As the emissivity value is increased from 0.25 to 1 it is noticed that the convective Nusselt number decreases to a greater degree for higher Rayleigh number i.e., 10^6 than for Ra = 10^3. For an increase in emissivity from 0.25 to 0.5 the total Nusselt number is increased by 17.9% for Ra = 10^3 and 27.0% for Ra = 10^6 for combined natural convection and radiation. Again, when the value of emissivity is increased from 0.75 to 1 it is observed that the total Nusselt increase by 14.6% for Ra = 10^3 and 27.1% for Ra = 10^6. Thus, we can see that for lower values of emissivity the value of Nusselt number is lowest, and maximum transfer of heat occurs when the value of emissivity is maximum i.e., ε = 1.

It is also evident that for an increase of emissivity from 0.25 to 1, the increase in total Nusselt number is found to be 24.9% and 97.1% respectively when compared with pure convection for Ra = 10^3. For Rayleigh number 10^6 the increase in Nusselt number is 32.6% and 170.9% sequentially when compared with pure convection.

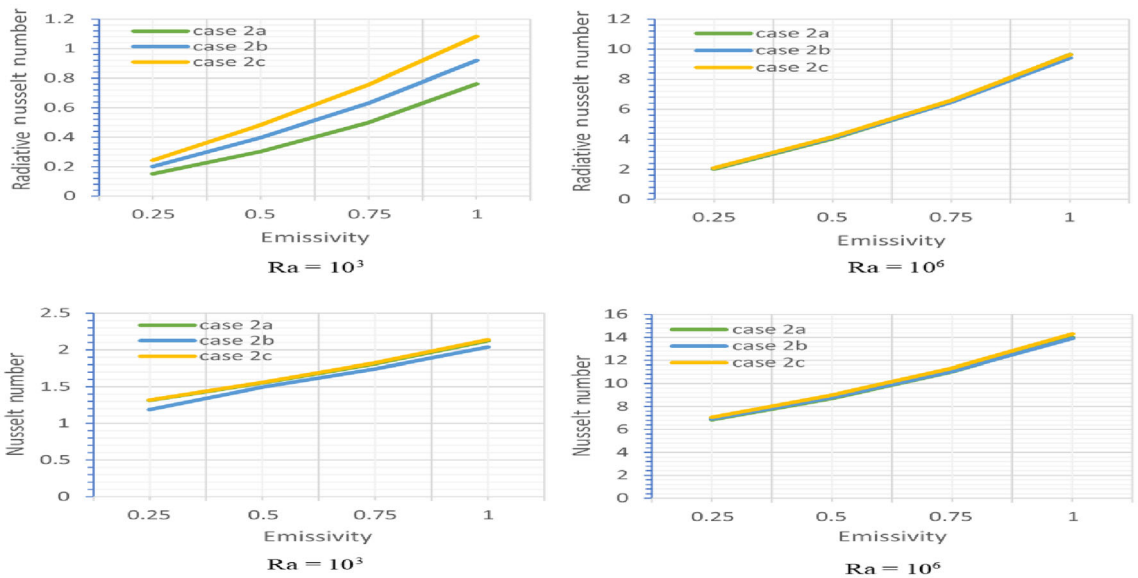

Figure 14. Variation of Radiative Nusselt number and Total average Nusselt number for hot wall with emissivity for Rayleigh number 10^3 and 10^6.

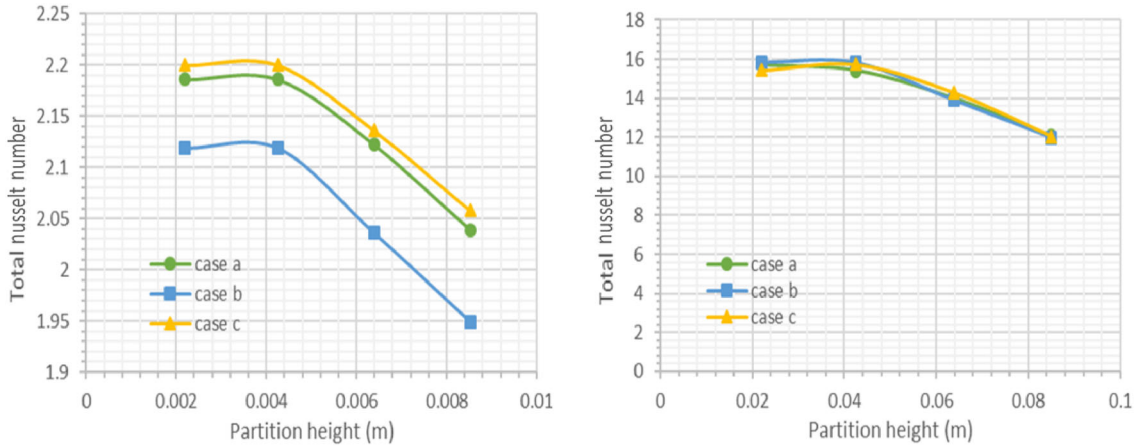

Figure 15. Variation of total Nusselt number with partition height for different partition distance for Rayleigh number 10^3 and 10^6 respectively.

4.5 *Effect of partition height*

Figure 15 shows the variation of total Nusselt number with partition height for Rayleigh number 10^3 and 10^6. Four cases of partition height are considered for the analysis. For the case 1 and 2 the height of the partition is h = L and 3L/4 respectively. For the case 3 and 4 two partitions are considered and the gap between them is taken as L/4 keeping 25% of the cavity open. In case 3 the stature of the partition attached to the top horizontal wall is of L/2 and for the one attached to bottom wall is of L/4. For case 4 the heights of upper and lower partitions are reversed, i.e., height of partition projected from top wall is L/4 and height of partition attached at bottom wall is L/2. By comparing the values of total Nusselt number for the hot wall for all the cases, it can be seen that the highest values of Nu_T are achieved when two partitions are considered having a gap between them as L/4, one partition is positioned at top wall and one at bottom wall i.e., for cases 3 and 4. Which is due to the fact that by decreasing the height of the partition more space is provided for fluid flow, thus causing more heat transfer.

The graph shows that the Nusselt number is least when the height of partition is highest and increases as the partition height is decreased for both the values of Rayleigh number. It is observed that when the height of partition is varied from h = L to L/4 for case 1 and 4 respectively, the value of Nusselt number increases to 7.2% for Ra 10^3 and 30.3% for Ra 10^6. Also, by comparing the values of total Nusselt number for the hot wall for all the cases as shown in graphs of figures 9, 10, 11 and 12 that the highest values

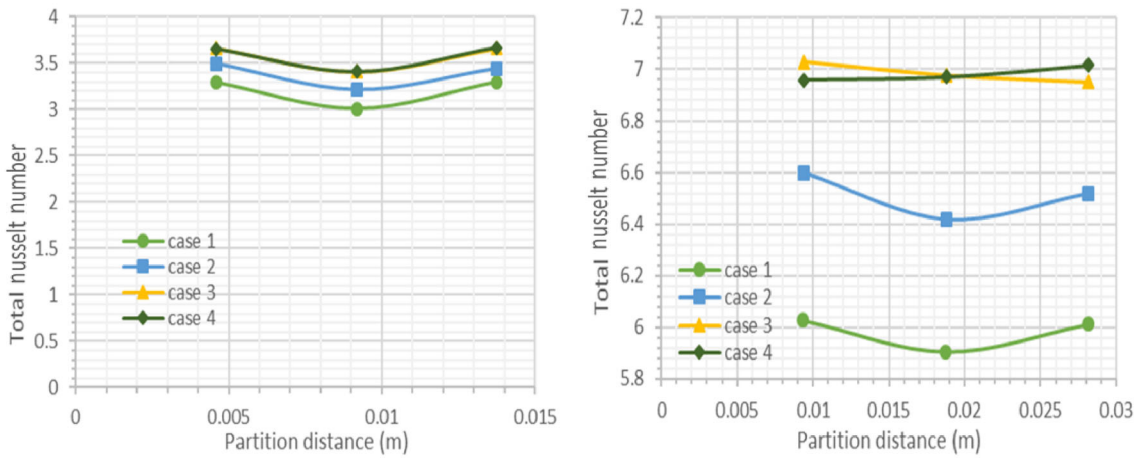

Figure 16. Variation of total Nusselt number with partition height for different partition distance for Rayleigh number 10^4 and 10^5.

of Nu_T are achieved when one partition is positioned at top wall and one at bottom wall i.e., for cases 3 and 4.

4.6 *Effect of partition distance*

In order to determine the effect of partition distance from hot wall on the combined natural convection and radiation phenomenon, three cases are considered 'a, b and c' for different partition distance and value of S_P for the cases is L/4, L/2 and 3L/4 respectively. In figure 16 variation of total Nusselt number for Ra = 10^4 and 10^5 respectively with the distance of partition from hot wall is presented. It is observed from the graph that value of Nusselt number is at a higher value when the partition is near the hot wall, decreases when placed at the centre and then increases when moved further away from hot wall and in closed proximity of cold wall. Again, from figures 9–12, the graphs shows that by comparing the three cases a, b and c it can be observed that the value of Nusselt number is increasing as the partition is moving away from the hot wall and least when placed at centre. Thus, the value of Nusselt number for Ra 10^3 to 10^6 is maximum for case 'c' when the distance of partition is 3L/4 for almost all the cases.

5. Conclusion

The combined laminar natural convection and radiation in a differentially heated square cavity with partition of different heights and distance from hot wall protruding on horizontal adiabatic walls are studied with the help of finite volume method. The prime investigation of the present work is to study the effect of radiation, position and stature of the partitions on natural convection and radiation within a square cavity for a range of Rayleigh number. Certain conclusions have been noted from the present research work which could be helpful for future research works. The inclusion of surface radiation effects the total heat transfer phenomenon in an enclosure with partition. The values of total Nusselt number are much higher for combined radiation and natural convection than for pure natural convection as can be observed for Ra 10^4 where the percentage increase in Nusselt number is 63.2%. It is observed that total Nusselt number increases after surface radiation interaction while the contribution of convective heat transfer decreases. It is also concluded that the average Nusselt number increases linearly as the Rayleigh number increases from 10^3 to 10^6 for all considerations of partition height and position. This happens because when Ra = 10^3, the natural convection flow is significantly low and the transfer of heat occurs essentially by conduction. As the Rayleigh number increases to 10^5 the convection currents along with interaction with surface radiation significantly enhances the heat transfer characteristics in the cavity. Further, increasing the Rayleigh number to 10^6 the effect of radiation dominates the heat transfer phenomenon. The lower values of Nusselt number along the hot wall are seen for case 1 and 2 when the height of the partition is L and 3L/4 respectively, as compared to rest of the cases leading to a conclusion that reduction in partition length results in higher rates of heat transfer and fluid flow. It is further observed that the Nusselt number varies with different values of emissivity in the cavity under study. In comparison, the total Nusselt number is achieved most in the case 'c' when the partition is farthest from the hot vertical wall, hence forming the conclusion that decreasing the length of partition distance from hot wall decreases the overall transfer of heat. Therefore, Nusselt number for a square cavity with partition placed at the extreme distance i.e., 3L/4 is greater than other partition positions.

References

[1] Nagaraja R A, Vijay Kumar V M and Seetharamu K N 2020 Natural convection in a square enclosure with partitions. *Mukt Shabd J.* 9: 7140–7147

[2] Almakhyoul Z M, Ali R A and Aldabbagh M S 2020 Effect of staggered non-conductive partition on heat transfer in a variable shape cavity. *Int. J. Mech. Prod.* 9: 381–390

[3] Parmananda M, Dalal A and Natarajan G 2018 The influence of partitions on predicting heat transfer due to the combined effects of convection and thermal radiation in cubical enclosures. *Int. J. Heat Mass Transf.* 121: 1179–1200

[4] Selamata M S and Hashimb I 2014 Effects of position of partitions on natural convection in squares enclosures. In: *AIP Conference Proceedings*, pp. 886–890

[5] Sathiyamoorthy M and Chamkha A J 2014 Analysis of natural convection in a square cavity with a thin partition for linearly heated side walls. *Int. J. Numer. Methods Heat Fluid Flow* 24: 1057–1072

[6] Saha S C and Gu Y T 2015 Transient air flow and heat transfer in a triangular enclosure with a conducting partition. *Appli. Math. Modell.* 10: 006

[7] Yamaguchi Y and Asako Y 2001 Effect of partition wall on natural convection heat transfer in a vertical air layer. *J. Heat Transf.* 123: 441–449

[8] Bilgen E 2002 Natural convection in enclosures with partial partitions. *Renew. Energy* 26: 257–270

[9] Khalifa A J N and Khudheyer A F 2001 Natural convection in partitioned enclosures: experimental study on 14 different configurations. *Energy Convers. Manag.* 42: 653–661

[10] Ramesh N and Venkateshan S P 1999 Effect of surface radiation and partition resistance on natural convection heat transfer in a partitioned enclosure: an experimental study. *J. Heat Transf.* 121: 616–622

[11] Karki K G, Sathyamurthy P S and Patankar S V 1992 Natural convection in a partitioned cubic enclosure. *J. Heat Transf.* 114: 410–417

[12] Ciofalo M and Karayiannis T G 1991 Natural convection heat transfer in a partially or completely-partitioned

vertical rectangular enclosure. *Int. J. Heat Mass Transfer*. 34: 167–179

[13] Khatamifar M, Lin W and Dong L 2021 Transient conjugate natural convection heat transfer in a differentially-heated square cavity with a partition of finite thickness and thermal conductivity. *Case Stud. Therm. Eng*. 25: 100952c

[14] Nansteel M W and Greif R 1981 Natural convection in undivided and partially divided rectangular enclosures. *J. Heat Transf.* 103: 623–629

[15] Kahveci K 2007 Numerical simulation of natural convection in a partitioned enclosure using PDQ method. *Int. J. Numer. Methods Heat Fluid Flow*. 17: 439–456

[16] Bejan A 2013 *Convection heat transfer*. Vol 4

[17] Howell J R, Mengüç M P and Siegel R 2020 *Thermal Radiation Heat Transfer*. Vol 7

[18] Bajorek S M and Lloyd J R 1982 Experimental investigation of natural confection in partitioned enclosures. *J. Heat Transf.* 104: 527–532